OXFORD

ORIGINAL ARTICLE

Multiscale Structure–Function Gradients in the Neonatal Connectome

Sara Larivière[1], Reinder Vos de Wael[1], Seok-Jun Hong[1,2], Casey Paquola[1], Shahin Tavakol[1], Alexander J. Lowe[1], Dewi V. Schrader[3] and Boris C. Bernhardt[1]

[1]Multimodal Imaging and Connectome Analysis Laboratory, McConnell Brain Imaging Centre, Montreal Neurological Institute and Hospital, McGill University, Montreal, QC H3A 2B4, Canada, [2]Center of the Developing Brain, Child Mind Institute, New York, NY 10022, USA and [3]BC Children's Hospital, Division of Neurology, Department of Pediatrics, University of British Columbia, Vancouver, BC V6H 3N1, Canada

Address correspondence to Boris C. Bernhardt, PhD and Sara Larivière, MSc, Montreal Neurological Institute (NW-256), 3801 University Street, Montreal, Quebec H3A 2B4, Canada. Email: boris.bernhardt@mcgill.ca. Email: sara.lariviere@mail.mcgill.ca

Abstract

The adult functional connectome is well characterized by a macroscale spatial gradient of connectivity traversing from unimodal toward higher-order transmodal cortices that recapitulates known principles of hierarchical organization and myelination patterns. Despite an emerging literature assessing connectome properties in neonates, the presence of connectome gradients and particularly their correspondence to microstructure remains largely unknown. We derived connectome gradients using unsupervised techniques applied to functional connectivity data from 40 term-born neonates. A series of cortex-wide analysis examined associations to magnetic resonance imaging-derived morphological parameters (cortical thickness, sulcal depth, curvature), measures of tissue microstructure (intracortical T1w/T2w intensity, superficial white matter diffusion parameters), and subcortico-cortical functional connectivity. Our findings indicate that the primary neonatal connectome gradient runs between sensorimotor and visual anchors and captures specific associations to cortical and superficial white matter microstructure as well as thalamo-cortical connectivity. A second gradient indicated an anterior-to-posterior asymmetry in macroscale connectivity alongside an immature differentiation between unimodal and transmodal areas, indicating a connectome-level circuitry en route to an adult-like organization. Our findings reveal an important coordination of structural and functional interactions in the neonatal connectome across spatial scales. Observed associations were replicable across individual neonates, suggesting consistency and generalizability.

Key words: connectomics, gradients, microstructure, neonates, neuroimaging

Introduction

The neonatal period is a time characterized by a fundamental change in the external environment and marks the beginning of extensive reconfigurations of structural and functional brain networks. *Post mortem* histological reports have demonstrated a surge in rapidly growing dendritic arborizations, myelination of axons in the cortex and superficial white matter, as well as in the accumulation of synaptic contacts especially in the period shortly after birth (Flechsig 1901; Huttenlocher 1979; Stiles and Jernigan 2010; Petanjek et al. 2011; Grayson and Fair 2017). While previous neuroimaging studies, particularly those

exploiting magnetic resonance imaging (MRI), have provided a rich catalogue of morphological and microstructural measures for the visualization of the neonatal brain *in vivo* (Knickmeyer et al. 2008; Yap et al. 2011; Ball et al. 2014), associations between neonatal brain structure and function remain largely unexplored.

Resting-state functional MRI (rs-fMRI) analyses offer noninvasive insights into the organization of functional systems in the absence of external tasks (Biswal et al. 1995; Fox et al. 2005), overcoming significant challenges in neonatal functional neuroimaging. Unlike work in adults, where functional network organization has been extensively investigated, principles governing neonatal connectome organization have been much less studied. Leveraging unsupervised decompositions of neonatal rs-fMRI data, multiple lines of research have suggested that canonical brain networks established in adults are also existent in neonates, yet with differences in their integration and differentiation from other networks (Fransson et al. 2007; Gao et al. 2009). Specifically, transmodal systems such as the default-mode and frontoparietal networks show rather sparse within-network connectivity, particularly between anterior and posterior components (Fransson et al. 2007; Lin et al. 2008; Gao et al. 2009). Several studies have complemented these findings by demonstrating that highly connected hubs are largely confined to primary visual and sensorimotor cortices (Fransson et al. 2011), a configuration that contrasts with the adult connectome organization, where central nodes are preferentially localized in transmodal association cortices (van den Heuvel and Sporns 2013). Extending beyond cortico-cortical connectivity, seed-based rs-fMRI studies in neonates have reported a dominance of thalamic connectivity on cortical function (Toulmin et al. 2015), likely reflecting the rapid and substantial growth in thalamo-cortical projections around birth (Kostovic and Jovanov-Milosevic 2006). While these findings point to a functional connectome organization that is uncharacteristic of adults and specific to neonates, the scarcity of work integrating *in vivo* functional and structural imaging contributes to an incomplete understanding of whether and how the neurostructural principles underlying macroscale functional topography at birth compares to adults.

We investigated cortico-cortical functional connectome organization in neonates, based on the first data release of the Developing Human Connectome Project (dHCP) (Makropoulos et al. 2018). To evaluate the interplay of cortical geometry and macroscale function, we employed unconstrained connectome compression techniques to visualize spatial trends in connectivity variations across the cortical surface. These techniques recapitulate macroscale cortical organization by situating every brain region along a continuous axis of differentiation in cortex-wide connectivity (Margulies et al. 2016; Guell et al. 2018; Mars et al. 2018). As such, they offer a framework to integrate macroscale functional connectomics with MRI-derived measures of cortical morphology and microstructure. In 40 term-born neonates, we showed a principal gradient of functional connectivity that was anchored in sensorimotor regions and radiated toward the visual cortex. Several cortex-wide analyses indicated specific associations to thalamo-cortical connectivity and measures of intracortical myelin, providing *in vivo* support for interactions between tissue microstructure, subcortical connectivity, and cortico-cortical connectome organization. Paralleling known hierarchical principles of the adult connectome (Margulies et al. 2016), we further observed a second, anterior-to-posterior connectivity gradient that closely followed variations in cortical thickness and differentiated between areas destined to become involved in transmodal processing, providing initial evidence of an immature higher-order circuitry en route to an adult-like organization.

Materials and Methods

Neonate Characteristics and Multimodal Imaging Dataset

We studied minimally preprocessed data from 40 term-born neonates (25 males; mean postmenstrual age at birth±SD: 39.0 ± 1.7 weeks; range 36–42 weeks, mean postmenstrual age at scan±SD: 39.9 ± 2.1 weeks) (Makropoulos et al. 2018). Data were downloaded from http://developingconnectome.org/ on 10/2017. Details on the MRI acquisition and image processing can be found in the Supplementary Materials. The data included multimodal MRI (3D T1-weighted MRI, 3D T2-weighted MRI, 2D rs-fMRI, and 2D diffusion-weighted MRI) acquired during natural sleep on a 3T Phillips Achieva with a dedicated neonatal imaging system. Downloaded data already underwent structural processing, involving motion correction, super-resolution reconstruction of the T1w and T2w images, and cortical surface reconstruction using the Medical Imaging Registration ToolKit (MIRTK) specifically adapted for neonatal MR data (Schuh et al. 2017; Makropoulos et al. 2018). For the rs-fMRI, preprocessing included correction for geometric distortions and head motion, band-pass filtering, and denoising (Fitzgibbon et al. 2017). Diffusion MRI preprocessing involved correction for (i) susceptibility distortions using FSL TOPUP (Andersson et al. 2003) and (ii) subject motion and eddy currents using FSL EDDY (Kuklisova-Murgasova et al. 2012; Andersson and Sotiropoulos 2016). Following upsampling to an isotropic resolution of 1.5 mm³, diffusion images were fed back to EDDY to correct for all distortions simultaneously (Bastiani et al. 2017).

Multimodal Data Fusion and Surface Registration

Based on surface-informed multimodal co-registrations (Greve and Fischl 2009), diffusion and rs-fMRI data were mapped to high-resolution T2w imaging space, which allowed for the aggregation of structural, functional, and diffusion features along cortical surface models of each individual. We constructed a sample-specific, hemisphere-unbiased surface template to register surface features into a common space. To this end, we first registered every subject's left and "flipped-right" native white matter mesh (*n* = 80) to a reference subject and averaged registered surfaces as an initial group template. We repeated this step 10 times, feeding the resulting template back as input into the following iteration. For computational efficiency, template surfaces and surface-registered features were downsampled to 5k vertices.

Functional Connectome Generation and Gradient Mapping

Neonatal Connectome Gradients

Following surface mapping, registration, and downsampling of cortical rs-fMRI time series, we computed pairwise correlations between each of the 5k cortical vertices to generate a functional connectome. The resulting matrix was *z*-transformed and averaged, resulting in a group-level connectome. We then applied diffusion map embedding, an unsupervised technique that identifies spatial axes in connectivity variation across

different areas (Coifman and Lafon 2006). In a recent application to adult functional connectomes, this technique revealed a gradient of connectivity variations that runs from unimodal (e.g., sensorimotor and visual cortices) to transmodal default-mode regions (Margulies et al. 2016). As in previous work (Margulies et al. 2016; Paquola et al. 2018; Vos de Wael et al. 2018; Hong et al. 2019), we retained only the top 10% of connections and converted the thresholded connectivity matrix into a normalized angle matrix, which scales the angle between each pair of vertices as a function of similarity. Manifold learning parameters were identical to those previously described, specifically $\alpha = 0.05$ and automated diffusion time estimation (Margulies et al. 2016). A MATLAB implementation of this algorithm is available at http://github.com/MICA-MNI/micaopen; the original Python code is available at http://github.com/satra/mapalign.

Comparison to the Adult Connectome Gradient
The adult connectome gradient was computed in a subsample of 100 young adults from the Human Connectome Project dataset (Van Essen et al. 2012) using the same procedure as described above and was surface-registered to the neonatal surface template. To address correspondence of the neonatal gradients with the adult gradient, we computed Spearman rank correlations between spatially matched nodes. Differences in gradients were further localized as the difference in rank at each node across the whole cortex.

Relation to MRI-Based Cortical Morphology and Microstructure

Cortical Morphology
Surface-registered mean curvature (the average of the principal curvatures, estimated from the white surface), sulcal depth (the change in position along the normal direction of a vertex, estimated during the inflation process), and cortical thickness (the Euclidean distance from a vertex on the white matter surface to its corresponding vertex on the pial surface) were provided for each neonate as part of the dHCP data release. While cortical thickness estimations in neonates may be challenging due to the prolonged existence of the subplate remnant at the gray–white matter interface (Kostovic et al. 2014), high-resolution MRI, together with intensity-based segmentation algorithms specifically adapted for neonatal brain MR images, generated accurate gray–white matter boundaries (rated independently by a neuroanatomist and a methods specialist), and thickness measurements comparable to those obtained from manually segmented cortices (Makropoulos et al. 2018). We used surface-wide linear models to examine associations between morphological features and functional gradients; statistical models were built using SurfStat for MATLAB (Worsley et al. 2009), available at http://www.math.mcgill.ca/~keith/surfstat.

MRI-Based Microstructure
We assessed microstructural organization in the neonatal brain using intracortical measures of T1w/T2 intensity and the analysis of diffusion tensor parameters in the superficial white matter. In adults, the analysis of intracortical T1w/T2w (Glasser and Van Essen 2011; Ganzetti et al. 2014) has provided spatial maps recapitulating earlier *post mortem* studies highlighting myeloarchitectonic differences between cortical areas (Flechsig 1901; Vogt 1910). Accordingly, for each

neonate, preprocessed T1w images were rigidly registered to the T2w image, and T1w/T2w intensity values were sampled at mid-thickness. As in previous work (Valk et al. 2016; Hong et al. 2018), we also generated surfaces probing the superficial white matter (i.e., the white matter ~2 mm beneath the gray–white matter interface) by systematically contracting the white matter interface along a Laplacian potential field toward the ventricular walls. A depth of 2 mm was chosen to target both termination zones of long-range tracts together with short-range U-fibers that arch through the cortical sulci to connect adjacent gyral regions (Schüz et al. 2002; Schmahmann and Pandya 2009). Following preprocessing of diffusion MRI (see Supplementary Materials), tensor-derived diffusion parameters fractional anisotropy (FA) and apparent diffusion coefficient (ADC), *in vivo* surrogates of fiber architecture and microstructure (Beaulieu 2002), were estimated using MRTrix[3] (v.0.3.15; http://www.mrtrix.org/) and subsequently interpolated along the superficial white matter surface. Lastly, T1w/T2w as well as diffusion-derived FA and ADC maps were registered to the surface template and surface-wide linear models assessed associations to functional gradients.

Relation to Subcortical Connectivity

Dominant connections between subcortical components—specifically the thalamus—and the cortex rapidly emerge at the time of normal birth and may play an influential role in shaping early macroscale functional organization (Rakic 1977; Kostovic and Rakic 1984; Toulmin et al. 2015). Specifically, the embedding of thalamo-cortical connections within a whole-brain corticocentric gradient approach can provide novel insights into the extent to which subcortical projections dictate cortical area identity at birth. To this end, we examined the role of subcortical regions on cortico-cortical functional organization and derived subcortico-cortical connectivity profiles for four subcortical structures (thalamus, lentiform nucleus, subthalamic nucleus, and caudate). Labels were initially based on the manually annotated neonatal brain atlases (Gousias et al. 2012) provided for each neonate as part of the dHCP (Makropoulos et al. 2014). We registered every neonate's structural image, label map, and functional data to a 40-week volumetric neonatal template (Serag et al. 2012), computed a mask of overlapping voxels for each structure, and extracted mean functional time series. For every neonate, Pearson correlation coefficient maps were calculated between each subcortical mask and each cortical vertex. Connectivity maps were z-scored, averaged across subjects, and correlated to the group-level functional gradients. To address specificity, we repeated the analysis after controlling for the other subcortical structures.

Robustness and Individual Analyses

Reproducibility Assessment in Individual Neonates
To assess consistency of our findings across individuals, we repeated the above analyses independently in each neonate. In each individual, we carried out a Procrustes rotation to align subject-specific gradients to the group-level gradient template (generated using all other 39 neonates). Neonate-specific associations between functional gradients were examined with individual MRI-based measures of cortical morphology (cortical
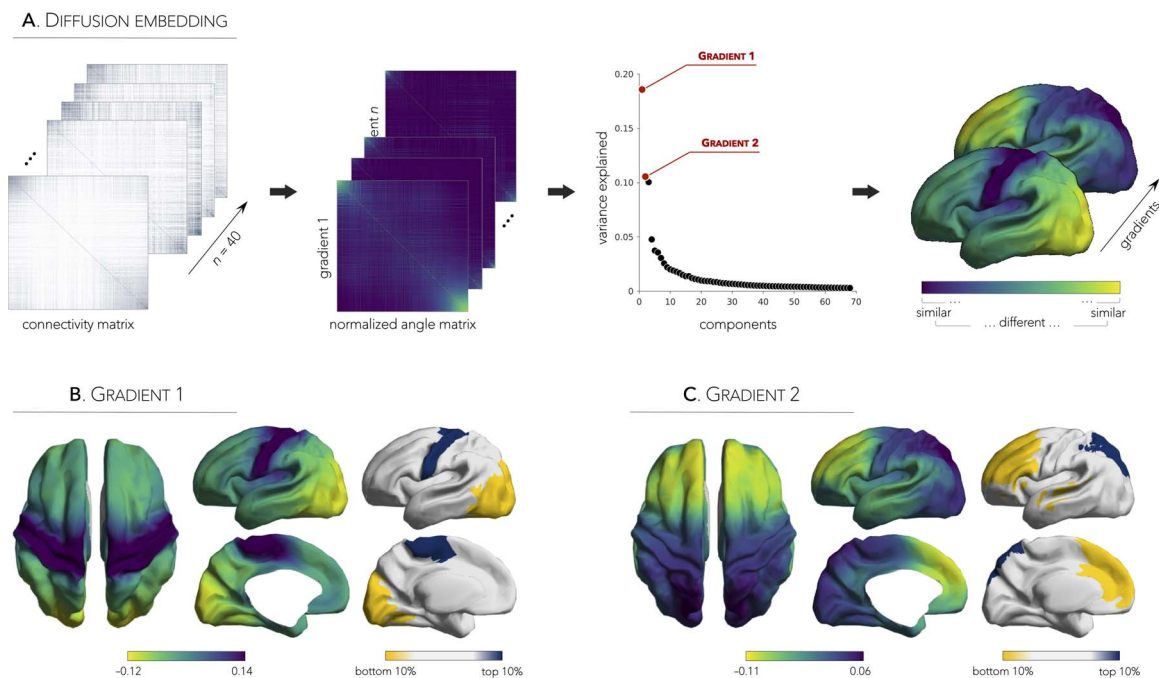
Figure 1. Diffusion embedding pipeline and neonatal connectome gradients. (A) The group-level connectivity matrix was transformed to a normalized angle matrix that expressed inter-areal similarity in connectivity profiles. Matrices were sorted by gradient values to highlight similarities (top-left/bottom-right corners) and differences (middle) in connectivity profiles. Components (i.e., gradient maps) explaining the principal axes of variance were extracted and mapped onto a sample-specific, hemisphere-unbiased neonatal surface template. Gradients of functional connectivity showing a dissociation between (B) sensorimotor and visual cortices (Gradient 1; G1) as well as between (C) posterior and anterior regions (Gradient 2; G2). Top and bottom 10% of the gradients highlight regions with similar (same color) and distinct (yellow vs. blue) connectivity profiles.

thickness), cortical microstructure (T1w/T2w), and superficial white matter diffusivity (FA, ADC) using linear models.

Matrix Thresholding
To verify that results were not biased by the choice of a threshold, functional connectome gradients and their associations to cortical morphology, microstructure, and subcortico-cortical connectivity were also computed using unthresholded connectivity matrices.

Results

We studied 40 term-born neonates from the openly shared developing human connectome project initiative (http://developingconnectome.org/) (Makropoulos et al. 2018). Using nonlinear manifold learning techniques, we derived functional connectivity gradients that depict spatial variations in connections when going from one cortical region to the next. Cortex-wide analyses then examined associations with (i) cortical morphology, (ii) microstructure, and (iii) subcortico-cortical connectivity patterns. Lastly, we evaluated consistency across individual neonates using reproducibility assessments.

Spatial Gradients Characterize Neonatal Connectome Variance

Using diffusion map embedding (Coifman and Lafon 2006), a nonlinear dimensionality reduction algorithm that sorts cortical areas based on their similarity in connectivity profiles, we identified two principal axes of functional connectivity variance in neonates (Fig. 1A). The first gradient (G1; Fig. 1B)

accounted for 19% of variance and differentiated sensorimotor from striate and extrastriate visual cortical areas, with regions located between the two extremes of G1 corresponding to frontal and parietal cortices. The second gradient (G2; Fig. 1C), on the other hand, accounted for 11% and appeared as a superposition of the adult default-mode network (Buckner et al. 2008; Spreng et al. 2010) while also showing a marked differentiation between anterior-to-posterior components (correlation with the anterior–posterior y-axis, $r = 0.79$). Cortex-wide nodal rank comparisons between the adult and neonatal gradients highlighted a strong negative association between the adult gradient and the anterior-to-posterior neonatal gradient (G2; $r = -0.69$), whereas a weaker association related the adult gradient to the sensorimotor-to-visual neonatal gradient (G1; $r = -0.17$; Supplementary Fig. 1A). Notably, maximal rank differences were observed in frontoparietal association areas (G_{adult} vs. $G1_{neonate}$) as well as in sensory cortices (G_{adult} vs. $G2_{neonate}$; Supplementary Fig. 1B).

Associations to MRI-Based Measures of Cortical Morphology and Microstructure

To identify structural substrates of macroscale connectivity gradients, we measured morphological (thickness, curvature, sulcal depth; Lerch et al. 2017) and microstructural (T1w/T2w intensity, a proxy for intracortical myelin, Glasser and Van Essen 2011; diffusion-derived FA and ADC) features shown to play a major role in structural maturation (Remer et al. 2017). High thickness was found predominantly in medial frontal regions, running from frontopolar to central areas as well as the temporoparietal cortex, while lower thickness was observed
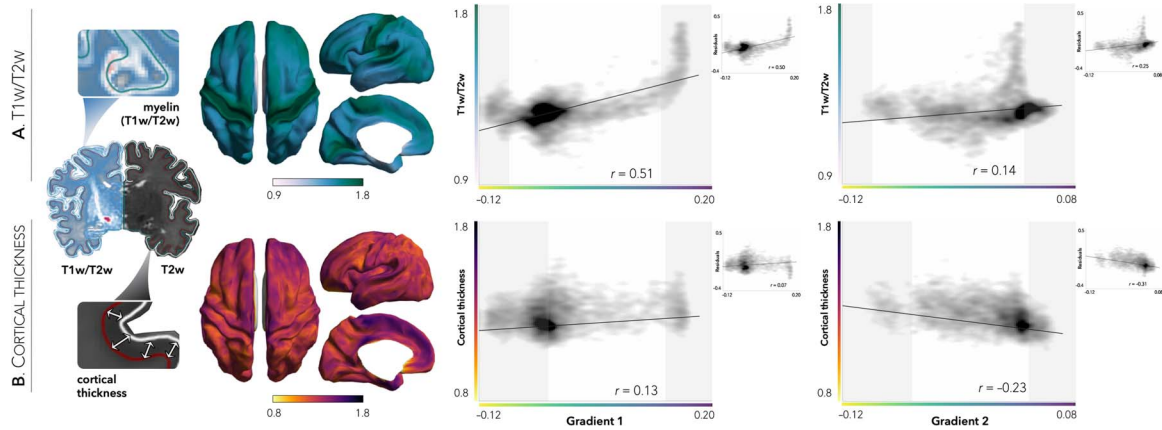
Figure 2. Associations between functional gradients and MRI-based measures of microstructure and cortical thickness. (A) T1w/T2w intensity, a proxy for intracortical myelin, was sampled at mid-thickness and mapped to the surface template (left). Highest values were observed at the sensorimotor extremity of G1—a finding that remained significant when controlling for cortical thickness (inset). (B) Cortical thickness, measured as the distance between the white matter and pial surfaces, was also mapped to the surface template (left). Correlations between connectivity gradients and cortical morphology revealed greater thickness in anterior regions of G2—an association that became stronger when controlling for T1w/T2w (inset). Shaded areas denote top and bottom 10% of gradient values (right).

posteriorly in the lateral superior parietal cortex. Intracortical T1w/T2w mapping indicated high myelination in sensorimotor, calcarine, and posterior superior temporal areas. Importantly, examining cortex-wide associations between connectivity gradients and MRI-based morphological and microstructural features, we observed marked and specific spatial associations between G1 and T1w/T2w ($r = 0.51$; controlling for cortical thickness: $r = 0.50$; Fig. 2A). In contrast to G1, G2 related to anterior-to-posterior shifts in cortical thickness ($r = -0.23$), an association that became stronger when controlling for T1w/T2w ($r = -0.31$; Fig. 2B). Neither G1 nor G2 correlated with cortical folding measures (curvature/sulcal depth; $r_{G1} = -0.04/-0.09$, $r_{G2} = -0.02/-0.05$), and the above correlations between G1 and T1w/T2w and G2 and thickness were not affected when controlling for them (Supplementary Fig. 2).

Extending our morphological and microstructural explorations, we probed the superficial white matter approximately 2 mm beneath the cortical interface (Fig. 3A) to investigate the "U-fiber" system arching the sulcal white matter to connect adjacent gyri (Schmahmann and Pandya 2009). As with T1w/T2w, superficial white matter diffusion metrics indicated high FA alongside low diffusivity primarily in sensorimotor and visual cortices, and accordingly showed a stronger association to G1 (FA/ADC; $r = 0.53/-0.75$) than G2 (FA/ADC; $r = -0.04/-0.20$; Fig. 3B).

Thalamo-Cortical Connectivity Underlies the Principal Gradient

Extending beyond a corticocentric approach, we derived the functional connectivity profiles of four subcortical structures to cortical areas and evaluated their spatial correspondence with cortico-cortical gradients (Fig. 4). Specifically, we extracted the mean functional time series of the thalamus as well as lentiform, subthalamic, and caudate nucleus and computed group-averaged, z-transformed Pearson correlations to every cortical vertex. While thalamus, lentiform, and subthalamic nucleus showed strongest connectivity to primary sensorimotor regions, the caudate showed strongest functional connections

to visual regions. Notably, although the former three subcortical connectivity profiles closely resembled G1 ($rs > 0.37$), only thalamo-cortical connectivity remained significantly positively correlated to G1 after controlling for the connectivity of the other structures ($r = 0.48$). Correlations between any subcortical structure and G2, on the other hand, remained weak ($rs < \pm 0.20$), even after controlling for the connectivity profiles of other structures ($rs < \pm 0.23$).

Findings Are Reproducible Across Individual Neonates

Reproducibility at the subject-level was assessed by repeating the above analyses in each neonate independently. Overall, individual-level cortical gradient maps were similar to the group-level gradients and consistent across neonates (mean $\pm$ SD: $r_{G1} = 0.63 \pm 0.14$, $r_{G2} = 0.52 \pm 0.15$; Fig. 5). As for the associations between cortico-cortical connectome gradients, subcortico-cortical connectivity as well as MRI-based morphological and microstructural features, highest stability was observed for the correlations between G1 and T1w/T2w (mean $\pm$ SD: $r = 0.30 \pm 0.12$), FA (mean $\pm$ SD: $r = 0.29 \pm 0.10$), as well as ADC (mean $\pm$ SD: $r = -0.34 \pm 0.12$). Lower stability was observed for correlations between G1 and subcortico-cortical connectivity (e.g. thalamo-cortical, mean $\pm$ SD: $r = 0.28 \pm 0.32$). Considering the association between cortical thickness and G2, correlations were low yet consistent (mean $\pm$ SD: $r = 0.04 \pm 0.04$).

Consistency Across Matrix Thresholds

Our results were robust when no initial thresholding was applied to the functional connectivity matrix. Specifically, functional connectome gradients as well as their associations to (i) cortical thickness, (ii) intracortical T1w/T2w intensity, (iii) superficial white matter markers (FA and ADC), and (iv) thalamo-cortical connectivity yielded similar results as our main findings (Supplementary Fig. 3).
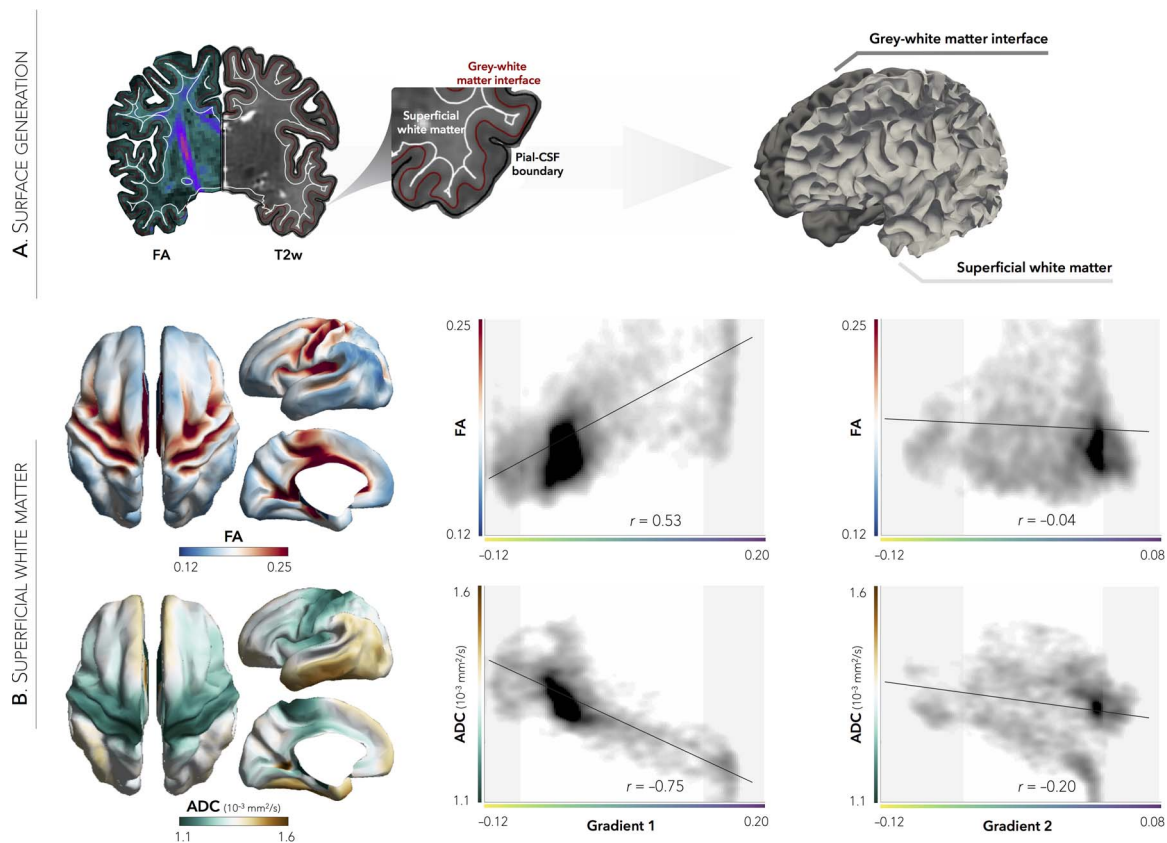
Figure 3. Correspondence of G1 to diffusion parameters in the superficial white matter. (A) FA and ADC were sampled from superficial white matter surfaces running 2 mm below the gray–white matter interface. (B) While G2 showed only marginal associations, G1 strongly correlated with FA and ADC, suggesting robust structure–function correspondence for sensorimotor and visual regions. Shaded areas denote top and bottom 10% of gradient values, respectively.

Discussion

Early postnatal brain development is a complex process involving a series of coordinated events affecting brain structure, wiring, and function. While structure–function interactions operate within highly constrained genetic contexts, these processes are also exposed to constantly changing external environments. The current work explored the multiscale coordination of structural and functional properties of term-born neonates *in vivo* by integrating macroscale functional connectomics with MRI-derived features of cortical morphology and tissue microstructure. By systematically analyzing variations in connectivity profiles along the cortical manifold, we provide novel and robust evidence for a principal macroscopic connectivity gradient running from sensorimotor to striate and extrastriate visual areas. Several cortex-wide analyses indicated specific associations to thalamo-cortical connectivity as well as T1w/T2w intensity, with the latter suggesting a spatial coupling of microstructural variations measurable at the scale of MRI and macroscale trends in neonatal connectome organization. Our findings further revealed a secondary axis of gradual connectivity shifts that described anterior-to-posterior variations as well as an immature differentiation between unimodal and transmodal areas, which was shown to consistently relate to the maturational trajectories of cortical thickness. Repeating our analyses across all neonates showed high consistency of the observed multiscale relationships,

suggesting generalizable interactions between neonatal brain structure and function.

Complementing clustering-based decompositions of the connectome into discrete communities (Power et al. 2011; Yeo et al. 2011), gradient mapping techniques capture continuous transitions between different functional systems along the folded cortical mantle, recapitulating spatial trends in sensorimotor hierarchies established in genetic manipulations during embryonic development (Hamasaki et al. 2004; Armentano et al. 2007). Mirroring intrinsic determinants of cortical patterning (O'Leary et al. 2007), our *in vivo* findings situated sensorimotor and visual networks at each apex of the principal neonatal gradient. Notably, this specific sensorimotor-to-visual encoding of position along the cortical axis reflects graded expression patterns of transcription factors that set up the basic areal plan for rostral motor and caudal visual cortices (Simeone et al. 1992; Bishop et al. 2000; Liu et al. 2000; Sahara et al. 2007). Aside from constraints of signaling gradients, the brain's functional architecture at birth is already set to allow for extrinsically mediated mechanisms, including thalamo-cortical input relaying continuous sensorimotor exploration of the outside world back to the cortex (O'Leary et al. 2007; Streri et al. 2013). In line with theories of developmental staging (Piaget 1970; Mandler 1988; Streri et al. 2013), the location of sensorimotor and visual regions as anchors of the primary functional gradient may prioritize communication within each of these specialized systems shortly after birth
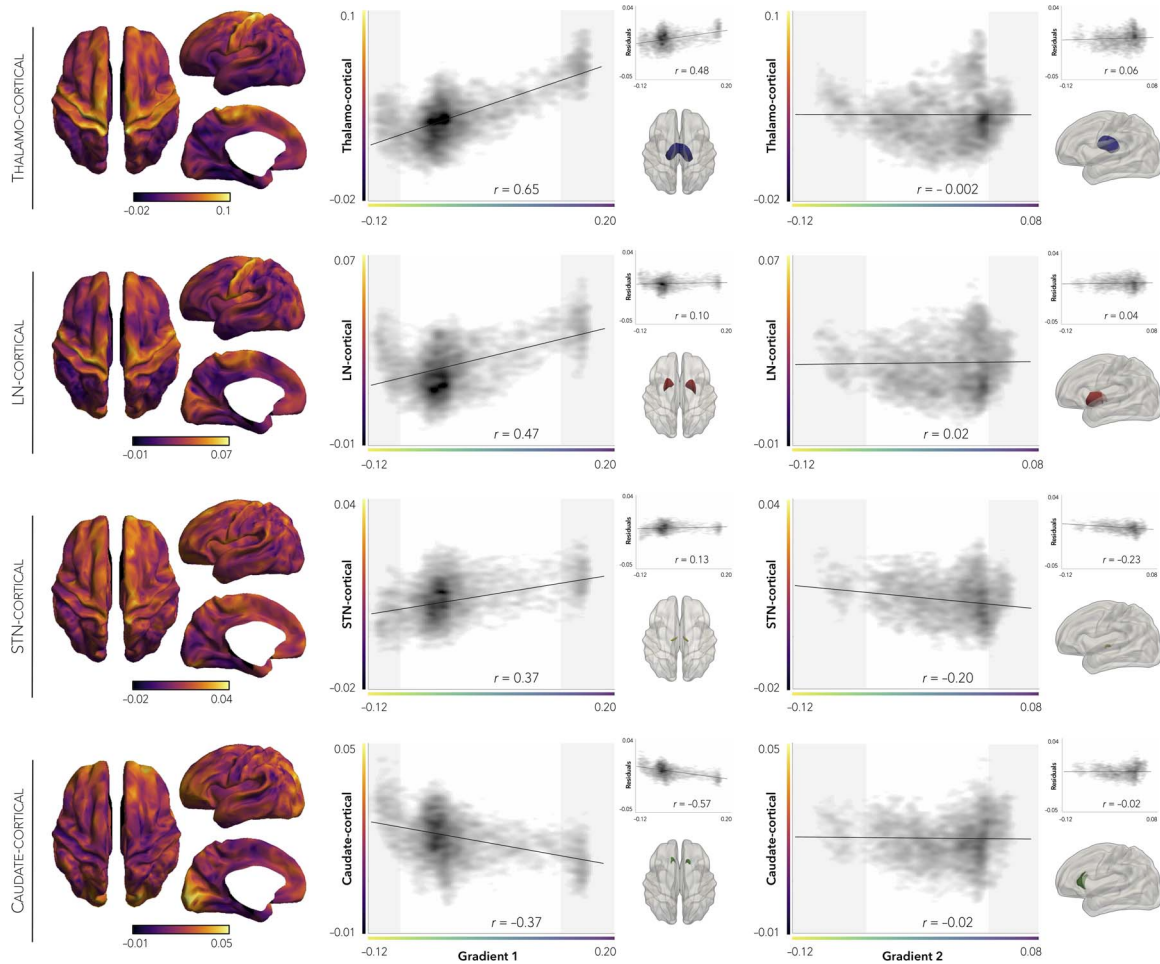
Figure 4. Thalamo-cortical connectivity underlies G1. Subcortico-cortical connectivity profiles of four subcortical structures all indicated preferential connectivity to sensorimotor (thalamus, lentiform nucleus, subthalamic nucleus) or visual (caudate) cortices (left panel). Systematic correlations between the subcortico-cortical maps and each macroscale gradient (right panel) showed maximal and specific associations between thalamo-cortical connectivity and G1 (top insets). Surface masks of each subcortical structure are displayed in the bottom insets. Shaded areas denote top and bottom 10% of gradient values, respectively.

(van den Heuvel and Sporns 2013). Interestingly, although the overall connectome organization in neonates stands in stark contrast to that observed in adults, which describe a unimodal-to-transmodal organization (Margulies et al. 2016; Huntenburg et al. 2017), the second neonatal gradient may actually reflect a rudimentary version of the principal gradient in adults. One plausible mechanism explaining this underdeveloped gradient is that functional maturation of higher-order networks is driven by the integration of distant regions, likely through a combination of synaptic pruning and strengthening of long-range connections along the anterior-to-posterior axis during early and late childhood (Huttenlocher and Dabholkar 1997; Dosenbach et al. 2010). Higher-order functional systems, specifically, sustain protracted changes during development (Petanjek et al. 2007), showing connectivity increases along the anterior–posterior dimension of the default-mode network together with the segregation of default-mode from frontoparietal networks—cortical circuits which will eventually form a transmodal apex as they transition to an adult configuration (Fair et al. 2009; Supekar et al. 2010; Margulies et al. 2016).

Leveraging a surface-based reference frame to visualize connectome gradients, we furthermore assessed the interplay between macroscale functional topographies and underlying structural properties. Interestingly, our analyses revealed diverging associations between the two principle functional gradients G1 and G2 and MRI-derived markers of cortical and subcortical microstructure as well as morphology. Indeed, spatial trends in G1 strongly resembled Flechsig's myelogenetic investigations of the *post mortem* human cortex, in which he described spatio-temporal profiles of cortical myelination as a function of the maturational trajectories of distinct functional systems (Flechsig 1901). Specifically, we observed that cortical regions situated at each extremity of G1, namely sensorimotor and visual cortices, coincide with Flechsig's "primordial areas" that are already myelinated at birth, while higher-order regions situated in-between the two extremities overlap with "terminal zones"—areas last to myelinate (Flechsig 1901). While our findings suggest that G1's sensorimotor-to-visual spatial connectivity profile may be modulated by cortical microstructure, and likely myeloarchitecture as measured at the scale of MRI, G2's anterior-to-posterior asymmetry rather reflects overall cortical thickness increases toward the frontal lobes and are believed to follow concurrent inside-out and rostro-caudal spatiotemporal gradients of neurogenesis and
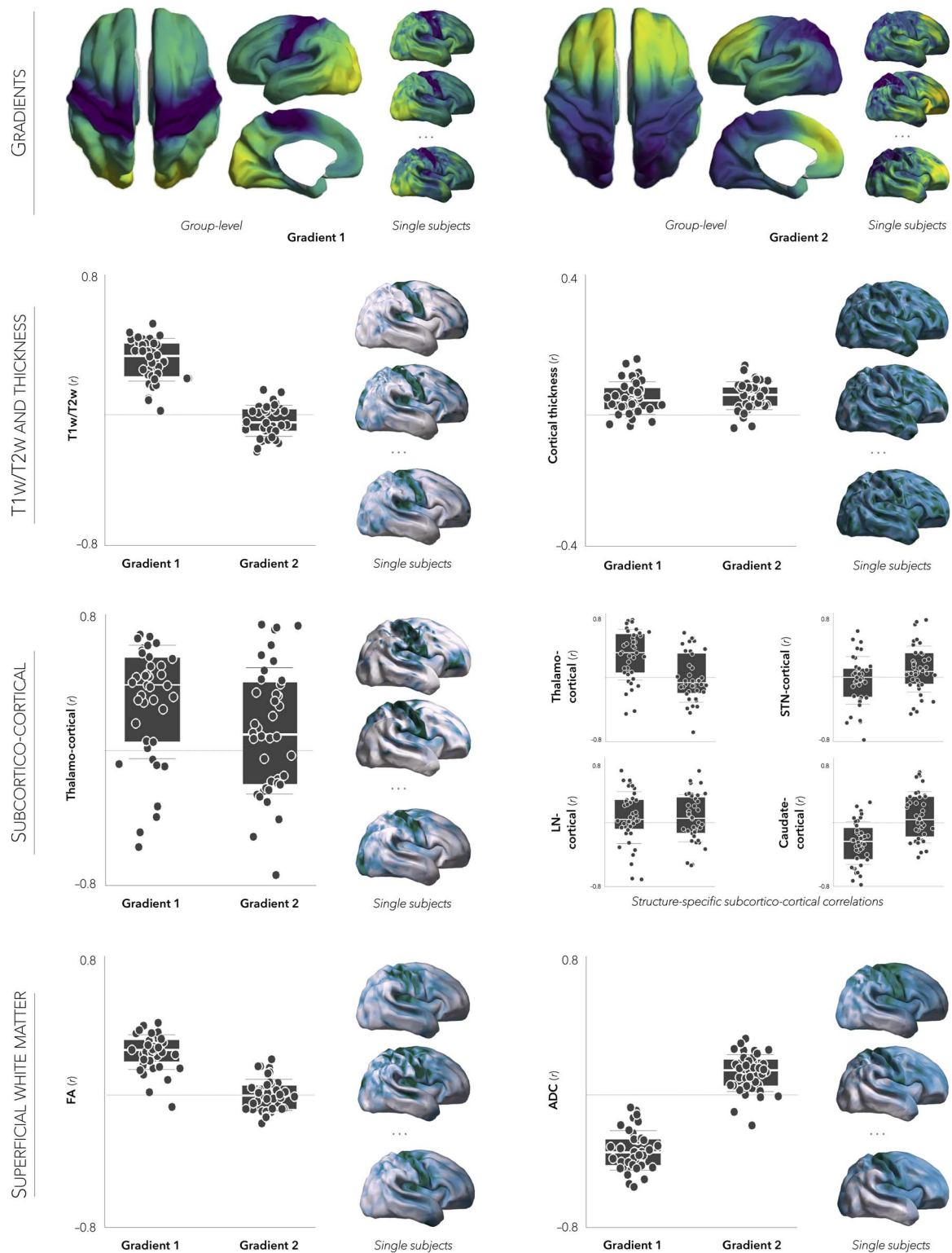
Figure 5. Reproducibility of findings across individual participants. Multiscale connectome analyses were repeated independently in each neonate. Box plots depict subject-specific Pearson correlation values between subcortico-cortical, structural, or superficial white matter features and each principal gradient. To show consistency in spatial patterns, individual feature maps for a subset of neonates are projected onto the surface template.

synaptogenesis (Sanderson and Weller 1990; Voigt et al. 1993). Indeed, the synaptic "big bang" occurring around birth, whereby the number of synapses increases to about 150% of that seen in adults (Huttenlocher 1979; Bourgeois 2010; Petanjek et al. 2011), is primarily stimulated by sensory input and represents an important phase in early connectome genesis (Rakic et al.

1986; Huttenlocher and Dabholkar 1997; Lagercrantz 2016). As synaptic processes are highly dependent on neuronal activity following birth (Peng et al. 2009), the neural processes underlying complex social, behavior, and cognitive processes have likely not matured by birth, a theory congruent with the fragmented higher-order regions observed in G2.

In addition to overarching functional, morphological, and microstructural principles of neonatal connectome organization, previous histological and functional neuroimaging reports have confirmed an important role for subcortical connectivity in early brain function (Allendoerfer and Shatz 1994; Kostovic and Jovanov-Milosevic 2006; Alcauter et al. 2014; Toulmin et al. 2015). In animal models, thalamo-cortical connections have been shown to fine-tune functional topographies prior to the onset of cortical sensory information processing, gradually configuring a "protomap" of cortical organization (Rakic 1988; Luhmann et al. 2009; Moreno-Juan et al. 2017). Our *in vivo* findings confirm that macroscale functional organization of the neonatal human cortex is measurably and specifically associated with thalamo-cortical projections. Thalamic afferents to the sensorimotor cortex represent important anchors in shaping neonatal functional organization, with most connections thought to originate from ventral lateral and posterolateral nuclei (Toulmin et al. 2015). In agreement with reports in healthy adults suggesting that areas of similar microstructural profiles are more likely to be interconnected and occupy a similar location along the cortical gradient (Huntenburg et al. 2017), the current work extended this "wiring rule" to the neonatal phase. We further showed that systematic associations underlying neonatal connectome organization extend beyond microstructural similarity, and encompass a combination of features across multiple scales, including cortical morphology as well as subcortico-cortical connectivity.

Comparative studies investigating the evolutionary divergence between humans and macaque monkeys have noted a spatial correspondence between areas undergoing postnatal cortical maturation, brain growth, and those showing an evolutionary expansion in surface area (Toro et al. 2008; Hill et al. 2010; Smaers et al. 2017). Interestingly, anterior and posterior brain areas located at each extremity of G2 correspond to regions of disproportionate evolutionary areal expansion; these also correspond to association cortices known to exhibit the greatest geodesic distance along the cortical mantle to primary sensory areas, providing a potential spatial substrate of increasing functional differentiation along the cortical hierarchy (Margulies et al. 2016). The phylogenetic increase in higher-order regions in humans is further reflected in the second neonatal connectome gradient, in which we observed a clear distinction between anterior and posterior transmodal cortices. Expansion of—and interactions among—these association areas are thought to be central to the evolution of human cognitive abilities, particularly for high-level competences in language, self-referential processing, and theory of mind (Uddin et al. 2007; Taylor et al. 2015; de Caso et al. 2017; Margulies and Smallwood 2017). Cellular and functional studies suggest that postnatal cortical expansion may be dominated by local variations in synaptic density, dendritic arborisation, and degree of myelination, and further demonstrated that high-expanding regions tend to be structurally and functionally less mature at birth than their low-expanding counterparts (Huttenlocher and Dabholkar 1997).

The early presence of multiscale interactions already evident in the first few days after birth brings about a novel view on connectome genesis and organization during development. Future studies, however, are needed to better characterize the transition of hierarchical gradients from mid-gestation to early childhood and adulthood. Ongoing open-access initiatives, such as the Developing Human Connectome Project dataset that the current work capitalized on, can provide the neuroimaging and network neuroscience communities with a 4-dimensional connectome of early life, including multimodal imaging, clinical, genetic, and behavioral data from 20 to 44 weeks postmenstrual age. A comprehensive understanding of the principles underlying connectome genesis will ultimately prove beneficial to devise sensitive markers of atypical network formation and maturation closely associated to multiple detrimental and lifelong neurodevelopmental conditions (Lariviere et al. 2018).

Supplementary Material

Supplementary material is available at: *Cerebral Cortex* online.

Funding

References

Alcauter S, Lin W, Smith JK, Short SJ, Goldman BD, Reznick JS, Gilmore JH, Gao W. 2014. Development of thalamocortical connectivity during infancy and its cognitive correlations. *J Neurosci*. 34:9067–9075.

Allendoerfer KL, Shatz CJ. 1994. The subplate, a transient neocortical structure: its role in the development of connections between thalamus and cortex. *Annu Rev Neurosci*. 17:185–218.

Andersson JL, Skare S, Ashburner J. 2003. How to correct susceptibility distortions in spin-echo echo-planar images: application to diffusion tensor imaging. *Neuroimage*. 20:870–888.

Andersson JLR, Sotiropoulos SN. 2016. An integrated approach to correction for off-resonance effects and subject movement in diffusion MR imaging. *Neuroimage*. 125:1063–1078.

Armentano M, Chou SJ, Tomassy GS, Leingartner A, O'Leary DD, Studer M. 2007. COUP-TFI regulates the balance of cortical patterning between frontal/motor and sensory areas. *Nat Neurosci*. 10:1277–1286.

Ball G, Aljabar P, Zebari S, Tusor N, Arichi T, Merchant N, Robinson EC, Ogundipe E, Rueckert D, Edwards AD et al. 2014. Rich-club organization of the newborn human brain. *Proc Natl Acad Sci U S A*. 111:7456–7461.

Bastiani M, Andersson JLR, Cordero-Grande L, Murgasova M, Hutter J, Price AN, Makropoulos A, Fitzgibbon SP, Hughes E, Rueckert D, *et al*. 2019. Automated processing pipeline for

neonatal diffusion MRI in the developing Human Connectome Project, *NeuroImage*. 185:750–763.

Beaulieu C. 2002. The basis of anisotropic water diffusion in the nervous system—a technical review. *NMR Biomed*. 15:435–455.

Bishop KM, Goudreau G, O'Leary DD. 2000. Regulation of area identity in the mammalian neocortex by Emx2 and Pax6. *Science*. 288:344–349.

Biswal B, Yetkin FZ, Haughton VM, Hyde JS. 1995. Functional connectivity in the motor cortex of resting human brain using echo-planar MRI. *Magn Reson Med*. 34:537–541.

Bourgeois J. 2010. The neonatal synaptic big bang. In: *The newborn brain: neuroscience and clinical applications*. Cambridge: Cambridge University Press, pp. 71–84

Buckner RL, Andrews-Hanna JR, Schacter DL. 2008. The brain's default network: anatomy, function, and relevance to disease. *Ann N Y Acad Sci*. 1124:1–38.

Coifman RR, Lafon S. 2006. Diffusion maps. *Appl Comput Harmon Anal*. 21:5–30.

de Caso I, Poerio G, Jefferies E, Smallwood J. 2017. That's me in the spotlight: neural basis of individual differences in self-consciousness. *Soc Cogn Affect Neurosci*. 12:1384–1393.

Dosenbach NU, Nardos B, Cohen AL, Fair DA, Power JD, Church JA, Nelson SM, Wig GS, Vogel AC, Lessov-Schlaggar CN *et al*. 2010. Prediction of individual brain maturity using fMRI. *Science*. 329:1358–1361.

Fair DA, Cohen AL, Power JD, Dosenbach NU, Church JA, Miezin FM, Schlaggar BL, Petersen SE. 2009. Functional brain networks develop from a "local to distributed" organization. *PLoS Comput Biol*. 5:e1000381.

Fitzgibbon S, Andersson J, Harrison S, Robinson E, Bozek J, Makropoulos A, Bastiani M, Griffanti L, Wright R, Schuh A, editors. 2017 The developing human connectome project automated functional pre-processing pipeline for neonates. *23rd Annual Meeting of the Organization for Human Brain Mapping*. Vancouver, Canada.

Flechsig PE. 1901. Developmental (myelogenetic) localisation of the cerebral cortex in the human subject. *Lancet*. 158:1027–1030.

Fox MD, Snyder AZ, Vincent JL, Corbetta M, Van Essen DC, Raichle ME. 2005. The human brain is intrinsically organized into dynamic, anticorrelated functional networks. *Proc Natl Acad Sci U S A*. 102:9673–9678.

Fransson P, Aden U, Blennow M, Lagercrantz H. 2011. The functional architecture of the infant brain as revealed by resting-state fMRI. *Cereb Cortex*. 21:145–154.

Fransson P, Skiold B, Horsch S, Nordell A, Blennow M, Lagercrantz H, Aden U. 2007. Resting-state networks in the infant brain. *Proc Natl Acad Sci U S A*. 104:15531–15536.

Ganzetti M, Wenderoth N, Mantini D. 2014. Whole brain myelin mapping using T1- and T2-weighted MR imaging data. *Front Hum Neurosci*. 8:671.

Gao W, Zhu H, Giovanello KS, Smith JK, Shen D, Gilmore JH, Lin W. 2009. Evidence on the emergence of the brain's default network from 2-week-old to 2-year-old healthy pediatric subjects. *Proc Natl Acad Sci U S A*. 106:6790–6795.

Glasser MF, Van Essen DC. 2011. Mapping human cortical areas in vivo based on myelin content as revealed by T1- and T2-weighted MRI. *J Neurosci*. 31:11597–11616.

Gousias IS, Edwards AD, Rutherford MA, Counsell SJ, Hajnal JV, Rueckert D, Hammers A. 2012. Magnetic resonance imaging of the newborn brain: manual segmentation of labelled atlases in term-born and preterm infants. *Neuroimage*. 62:1499–1509.

Grayson DS, Fair DA. 2017. Development of large-scale functional networks from birth to adulthood: a guide to the neuroimaging literature. *Neuroimage*. 160:15–31.

Greve DN, Fischl B. 2009. Accurate and robust brain image alignment using boundary-based registration. *Neuroimage*. 48:63–72.

Guell X, Schmahmann JD, Gabrieli J, Ghosh SS. 2018. Functional gradients of the cerebellum. *Elife*. 7:e36652.

Hamasaki T, Leingartner A, Ringstedt T, O'Leary DD. 2004. EMX2 regulates sizes and positioning of the primary sensory and motor areas in neocortex by direct specification of cortical progenitors. *Neuron*. 43:359–372.

Hill J, Inder T, Neil J, Dierker D, Harwell J, Van Essen D. 2010. Similar patterns of cortical expansion during human development and evolution. *Proc Natl Acad Sci U S A*. 107: 13135–13140.

Hong S, Hyung B, Paquola C, Bernhardt BC. 2018. The superficial white matter in autism and its role in atypical functional connectivity and symptom severity. *Cereb Cortex*. doi: 10.1093/cercor/bhy321 in press.

Hong S, Vos de Wael R, Lariviere S, Paquola C, Bethlehem R, Di Martino A, Milham MP, Margulies D, Smallwood J, Bernhardt BC, *et al*. 2019. Atypical functional connectome hierarchy in autism. *Nat Commun*. 10(1):1022.

Huntenburg JM, Bazin PL, Goulas A, Tardif CL, Villringer A, Margulies DS. 2017. A systematic relationship between functional connectivity and intracortical myelin in the human cerebral cortex. *Cereb Cortex*. 27:981–997.

Huttenlocher PR. 1979. Synaptic density in human frontal cortex—developmental changes and effects of aging. *Brain Res*. 163:195–205.

Huttenlocher PR, Dabholkar AS. 1997. Regional differences in synaptogenesis in human cerebral cortex. *J Comp Neurol*. 387:167–178.

Knickmeyer RC, Gouttard S, Kang C, Evans D, Wilber K, Smith JK, Hamer RM, Lin W, Gerig G, Gilmore JH. 2008. A structural MRI study of human brain development from birth to 2 years. *J Neurosci*. 28:12176–12182.

Kostovic I, Jovanov-Milosevic N. 2006. The development of cerebral connections during the first 20–45 weeks' gestation. *Semin Fetal Neonatal Med*. 11:415–422.

Kostovic I, Jovanov-Milosevic N, Rados M, Sedmak G, Benjak V, Kostovic-Srzentic M, Vasung L, Culjat M, Rados M, Huppi P *et al*. 2014. Perinatal and early postnatal reorganization of the subplate and related cellular compartments in the human cerebral wall as revealed by histological and MRI approaches. *Brain Struct Funct*. 219:231–253.

Kostovic I, Rakic P. 1984. Development of prestriate visual projections in the monkey and human fetal cerebrum revealed by transient cholinesterase staining. *J Neurosci*. 4:25–42.

Kuklisova-Murgasova M, Quaghebeur G, Rutherford MA, Hajnal JV, Schnabel JA. 2012. Reconstruction of fetal brain MRI with intensity matching and complete outlier removal. *Med Image Anal*. 16:1550–1564.

Lagercrantz H. 2016. Connecting the brain of the child from synapses to screen-based activity. *Acta Paediatr*. 105:352–357.

Lariviere S, Vos de Wael R, Paquola C, Hong SJ, Misic B, Bernasconi N, Bernasconi A, Bonilha L, Bernhardt B. 2018. Microstructure-informed connectomics: enriching large-scale descriptions of healthy and diseased brains. *Brain Connect*. 9:113–127. doi: 10.1089/brain.2018.0587 in press.

Lerch JP, van der Kouwe AJ, Raznahan A, Paus T, Johansen-Berg H, Miller KL, Smith SM, Fischl B, Sotiropoulos SN. 2017. Studying neuroanatomy using MRI. *Nat Neurosci*. 20:314–326.

Lin W, Zhu Q, Gao W, Chen Y, Toh CH, Styner M, Gerig G, Smith JK, Biswal B, Gilmore JH. 2008. Functional connectivity MR imaging reveals cortical functional connectivity in the developing brain. *AJNR Am J Neuroradiol*. 29: 1883–1889.

Liu Q, Dwyer ND, O'Leary DD. 2000. Differential expression of COUP-TFI, CHL1, and two novel genes in developing neocortex identified by differential display PCR. *J Neurosci*. 20:7682–7690.

Luhmann HJ, Kilb W, Hanganu-Opatz IL. 2009. Subplate cells: amplifiers of neuronal activity in the developing cerebral cortex. *Front Neuroanat*. 3:19.

Makropoulos A, Gousias IS, Ledig C, Aljabar P, Serag A, Hajnal JV, Edwards AD, Counsell SJ, Rueckert D. 2014. Automatic whole brain MRI segmentation of the developing neonatal brain. *IEEE Trans Med Imaging*. 33:1818–1831.

Makropoulos A, Robinson EC, Schuh A, Wright R, Fitzgibbon S, Bozek J, Counsell SJ, Steinweg J, Vecchiato K, Passerat-Palmbach J et al. 2018. The developing human connectome project: a minimal processing pipeline for neonatal cortical surface reconstruction. *Neuroimage*. 173:88–112.

Mandler JM. 1988. How to build a baby: on the development of an accessible representation system. *Cogn Dev*. 3:113–136.

Margulies DS, Ghosh SS, Goulas A, Falkiewicz M, Huntenburg JM, Langs G, Bezgin G, Eickhoff SB, Castellanos FX, Petrides M et al. 2016. Situating the default-mode network along a principal gradient of macroscale cortical organization. *Proc Natl Acad Sci U S A*. 113:12574–12579.

Margulies DS, Smallwood J. 2017. Converging evidence for the role of transmodal cortex in cognition. *Proc Natl Acad Sci U S A*. 114:12641–12643.

Mars RB, Passingham RE, Jbabdi S. 2018. Connectivity fingerprints: from areal descriptions to abstract spaces. *Trends Cogn Sci*. 22(11).

Moreno-Juan V, Filipchuk A, Anton-Bolanos N, Mezzera C, Gezelius H, Andres B, Rodriguez-Malmierca L, Susin R, Schaad O, Iwasato T et al. 2017. Prenatal thalamic waves regulate cortical area size prior to sensory processing. *Nat Commun*. 8:14172.

O'Leary DD, Chou SJ, Sahara S. 2007. Area patterning of the mammalian cortex. *Neuron*. 56:252–269.

Paquola C, Vos de Wael R, Wagstyl K, Bethlehem R, Seidlitz J, Hong S, Bullmore ET, Evans AC, Misic B, Margulies DS, Smallwood J, Bernhardt BC. 2018. Dissociations between microstructural and functional hierarchies within regions of transmodal cortex. bioRxiv. https://doi.org/10.1101/488700.

Peng YR, He S, Marie H, Zeng SY, Ma J, Tan ZJ, Lee SY, Malenka RC, Yu X. 2009. Coordinated changes in dendritic arborization and synaptic strength during neural circuit development. *Neuron*. 61:71–84.

Petanjek Z, Judaš M, Kostović I, HBJCc U. 2007. Lifespan alterations of basal dendritic trees of pyramidal neurons in the human prefrontal cortex: a layer-specific pattern. *Cereb Cortex*. 18:915–929.

Petanjek Z, Judas M, Simic G, Rasin MR, Uylings HB, Rakic P, Kostovic I. 2011. Extraordinary neoteny of synaptic spines in the human prefrontal cortex. *Proc Natl Acad Sci U S A*. 108:13281–13286.

Piaget J. 1970. *Piaget's theory* In P.H. Mussen (Ed.), Carmichael's handbook of child development (pp. 703–732). New York: Wiley.

Power JD, Cohen AL, Nelson SM, Wig GS, Barnes KA, Church JA, Vogel AC, Laumann TO, Miezin FM, Schlaggar BL et al. 2011. Functional network organization of the human brain. *Neuron*. 72:665–678.

Rakic P. 1977. Prenatal development of the visual system in rhesus monkey. *Philos Trans R Soc Lond B Biol Sci*. 278(961):245–246.

Rakic P. 1988. Specification of cerebral cortical areas. *Science*. 241:170–176.

Rakic P, Bourgeois JP, Eckenhoff MF, Zecevic N, Goldman-Rakic PS. 1986. Concurrent overproduction of synapses in diverse regions of the primate cerebral cortex. *Science*. 232: 232–235.

Remer J, Croteau-Chonka E, Dean DC 3rd, D'Arpino S, Dirks H, Whiley D, Deoni SCL. 2017. Quantifying cortical development in typically developing toddlers and young children, 1-6 years of age. *Neuroimage*. 153:246–261.

Sahara S, Kawakami Y, Izpisua Belmonte JC, O'Leary DD. 2007. Sp8 exhibits reciprocal induction with Fgf8 but has an opposing effect on anterior-posterior cortical area patterning. *Neural Dev*. 2:10.

Sanderson KJ, Weller WL. 1990. Gradients of neurogenesis in possum neocortex. *Brain Res Dev Brain Res*. 55:269–274.

Schmahmann J, Pandya D. 2009. *Fiber pathways of the brain*. USA: OUP.

Schuh A, Makropoulos A, Wright R, Robinson EC, Tusor N, Steinweg J, Hughes E, Grande LC, Price A, Hutter J, 2017. A deformable model for the reconstruction of the neonatal cortex. in *IEEE 14th International Symposium on Biomedical Imaging (ISBI)* pp. 800–803.

Schüz A, Braitenberg V. 2002. The human cortical white matter: quantitative aspects of cortico-cortical long-range connectivity. in: *Cortical Areas: Unity and Diversity* (eds. Schüz A. & Miller R.), Taylor & Francis, London, pp. 377–384.

Serag A, Aljabar P, Ball G, Counsell SJ, Boardman JP, Rutherford MA, Edwards AD, Hajnal JV, Rueckert D. 2012. Construction of a consistent high-definition spatio-temporal atlas of the developing brain using adaptive kernel regression. *Neuroimage*. 59:2255–2265.

Simeone A, Acampora D, Gulisano M, Stornaiuolo A, Boncinelli E. 1992. Nested expression domains of four homeobox genes in developing rostral brain. *Nature*. 358:687–690.

Smaers JB, Gomez-Robles A, Parks AN, Sherwood CC. 2017. Exceptional evolutionary expansion of prefrontal cortex in great apes and humans. *Curr Biol*. 27:1549.

Spreng RN, Stevens WD, Chamberlain JP, Gilmore AW, Schacter DL. 2010. Default network activity, coupled with the frontoparietal control network, supports goal-directed cognition. *Neuroimage*. 53:303–317.

Stiles J, Jernigan TL. 2010. The basics of brain development. *Neuropsychol Rev*. 20:327–348.

Streri A, de Hevia MD, Izard V, Coubart A. 2013. What do we know about neonatal cognition? *Behav Sci (Basel)*. 3:154–169.

Supekar K, Uddin LQ, Prater K, Amin H, Greicius MD, Menon V. 2010. Development of functional and structural connectivity within the default mode network in young children. *Neuroimage*. 52:290–301.

Taylor P, Hobbs JN, Burroni J, Siegelmann HT. 2015. The global landscape of cognition: hierarchical aggregation as an organizational principle of human cortical networks and functions. *Sci Rep*. 5:18112.

Toro R, Perron M, Pike B, Richer L, Veillette S, Pausova Z, Paus T. 2008. Brain size and folding of the human cerebral cortex. *Cereb Cortex*. 18:2352–2357.

Toulmin H, Beckmann CF, O'Muircheartaigh J, Ball G, Nongena P, Makropoulos A, Ederies A, Counsell SJ, Kennea N, Arichi T *et al*. 2015. Specialization and integration of functional thalamocortical connectivity in the human infant. *Proc Natl Acad Sci U S A*. 112:6485–6490.

Uddin LQ, Iacoboni M, Lange C, Keenan JP. 2007. The self and social cognition: the role of cortical midline structures and mirror neurons. *Trends Cogn Sci*. 11:153–157.

Valk SL, Bernhardt BC, Bockler A, Kanske P, Singer T. 2016. Substrates of metacognition on perception and metacognnition on higher-order cognition relate to different subsystems of the mentalizing network. *Hum Brain Mapp*. 37: 3388–3399.

van den Heuvel MP, Sporns O. 2013. Network hubs in the human brain. *Trends Cogn Sci*. 17:683–696.

Van Essen DC, Ugurbil K, Auerbach E, Barch D, Behrens T, Bucholz R, Chang A, Chen L, Corbetta M, Curtiss SWJN. 2012. The Human Connectome Project: a data acquisition perspective. *NeuroImage*. 62:2222–2231.

Vogt O. 1910. Die myeloarchitektonische Felderung des menschlichen Stirnhirns. *J Psychol Neurol*. 15:221–232.

Voigt T, De Lima AD, Beckmann M. 1993. Synaptophysin immunohistochemistry reveals inside-out pattern of early synaptogenesis in ferret cerebral cortex. *J Comp Neurol*. 330:48–64.

Vos de Wael R, Larivière S, Caldairou B, Hong S, Jefferies E, Margulies DS, Smallwood J, Bernasconi N, Bernhardt BC. 2018. Anatomical and microstructural determinants of hippocampal subfield functional connectome embedding. *Proc Natl Sci U S A*. 115(40):10154–10159.

Worsley KJ, Taylor J, Carbonell F, Chung M, Duerden E, Bernhardt B, Lyttelton O, Boucher M, Evans A, editors. 2009. A Matlab toolbox for the statistical analysis of univariate and multivariate surface and volumetric data using linear mixed effects models and random field theory. *Proceedings of the 15th Annual Meeting of the Organization for Human Brain Mapping*, 2009, San Francisco (CA): NeuroImage.

Yap PT, Fan Y, Chen Y, Gilmore JH, Lin W, Shen D. 2011. Development trends of white matter connectivity in the first years of life. *PLoS One*. 6:e24678.

Yeo BT, Krienen FM, Sepulcre J, Sabuncu MR, Lashkari D, Hollinshead M, Roffman JL, Smoller JW, Zollei L, Polimeni JR *et al*. 2011. The organization of the human cerebral cortex estimated by intrinsic functional connectivity. *J Neurophysiol*. 106:1125–1165.